This article was published in Colloids and Surfaces B: Biointerfaces, 123, 1-7, 2014
http://dx.doi.org/10.1016/j.colsurfb.2014.08.016

The effects of surface properties on *Escherichia coli* adhesion are modulated by shear stress

J.M.R. Moreira[a], J.D.P. Araújo[b], J.M. Miranda[b], M. Simões[a], L.F. Melo[a], F.J. Mergulhão[a]

[a] LEPABE – Department of Chemical Engineering, Faculty of Engineering, University of Porto, Rua Dr. Roberto Frias s/n 4200-465 Porto, Portugal

[b] CEFT – Department of Chemical Engineering, Faculty of Engineering, University of Porto, Rua Dr. Roberto Frias s/n 4200-465 Porto, Portugal

Correspondence: Filipe J. M. Mergulhão, Chemical Engineering Department, Faculty of Engineering University of Porto, Rua Dr. Roberto Frias, 4200-465 Porto, Portugal. Phone: (+351) 225081668. Fax: (+351) 5081449. E-mail: filipem@fe.up.pt.

Abstract

The adhesion of *Escherichia coli* to glass and polydimethylsiloxane (PDMS) at different flow rates (between 1 and 10 $ml.s^{-1}$) was monitored in a parallel plate flow chamber in order to understand the effect of surface properties and hydrodynamic conditions on adhesion. Computational fluid dynamics was used to assess the applicability of this flow chamber in the simulation of the hydrodynamics of relevant biomedical systems. Wall shear stresses between 0.005 and 0.07 Pa were obtained and these are similar to those found in the circulatory, reproductive and urinary systems. Results demonstrate that *E. coli* adhesion to hydrophobic PDMS and hydrophilic glass surfaces is modulated by shear stress with surface properties having a stronger effect at the lower and highest flow rates tested and with negligible effects at intermediate flow rates. These findings suggest that when expensive materials or coatings are selected to produce biomedical devices, this choice should take into account the physiological hydrodynamic conditions that will occur during the utilization of those devices.

Keywords: Bacterial adhesion, *Escherichia coli*, parallel plate flow chamber, PDMS, shear stress, hydrophobicity

Introduction

Bacteria often adhere to surfaces and form biological communities called biofilms [1] that develop in almost all types of biomedical devices [2]. These sessile cells are typically more resistant to antimicrobial agents than planktonic ones, have a decreased susceptibility to host defense systems and function as a source of resistant microorganisms responsible for many hospital acquired infections [3]. Moreover, biofilm spreading on the surface upon prolonged use of the biomedical device can cause

material biodegradation, changes in surface properties and deterioration of the medical functionality [1, 2].

Different polymers are commonly employed in biomedical devices. These materials should be biocompatible and have to be stable, resistant against different body fluids and display anti adhesive properties towards microorganisms [1-3]. Polydimethylsiloxane (PDMS) is a polymer that has been widely used in biomedical devices like contact lenses, breast implants, catheters, and used in the correction of vesico ureteric reflux in the bladder [1, 4]. These devices are often colonized by single bacterial species like *Escherichia coli* [5]. *E. coli* is responsible for 80% of the urinary tract infections and it was observed that even after antibiotic therapy it can persist and re-emerge in the bladder and in associated urinary tract biomedical devices (eg urinary catheters) [3, 6, 7]. *E. coli* has also been found in breast implants, being responsible for 1.5% of associated infections, and contact lenses [3, 8]. It has been reported that 60-70% of the hospital acquired infections are associated with medical devices and cost $5 billion annually in the US [9, 10]. Additionally, the costs associated with the replacement of infected implants during revision surgery may triple the cost of the primary implant procedure [11]. Moreover, secondary implants and devices have a higher infection incidence because antibiotic resistant bacteria residing in the surrounding tissue can proliferate and colonize the recently implanted device [11]. Therefore, owing to the problems associated with the increasing use of these devices, a preventive strategy must be adopted [3]. Understanding biofilm formation mechanisms and the factors that influence cell attachment to a surface is essential to prevent and to treat biofilm related diseases. The properties of microbial cells and environmental factors such as surface properties of the biomaterials as well as associated flow conditions affect the process of biofilm formation [12].

In vitro systems have been employed to test the effect of different surfaces on the

biofilm formation process under different environmental conditions [13]. Barton, et al. [14] have used a parallel plate flow chamber (PPFC) at a shear rate of 1.9 s^{-1} to observe the adhesion of *Staphylococcus epidermidis*, *Pseudomonas aeruginosa*, and *E. coli* to orthopedic implant polymers. These authors verified that *P. aeruginosa* adhered more than *S. epidermidis* and that the estimated values of the free energy of adhesion correlated with the amount of adherent cells. Pratt-Terpstra, et al. [15] developed a flow cell system to study the adhesion of three strains of oral streptococci to glass, cellulose acetate and a fluorethylenepropylene copolymer at a shear rate of 21 s^{-1}. They verified that a linear correlation was found between the number of bacteria adhering to those surfaces and the free energy of adhesion. Bruinsma, et al. [16] used a PPFC at a shear rate of 10 s^{-1} to study the adhesion of a hydrophobic *P. aeruginosa* and hydrophilic *Staphylococcus aureus* to hydrophobic and hydrophilic hydrogel contact lenses (CL) with and without an adsorbed tear film. The authors observed that adhesion of *P. aeruginosa* was more extensive than *S. aureus* although no difference between hydrophobic and hydrophilic CL was found. Millsap, et al. [17] studied the effect of a hydrophobic silicone rubber and a hydrophilic glass in the adhesion of six *Lactobacillus* strains using a PPFC at a shear rate of 15 s^{-1}. These authors have also concluded that adhesion to the tested surfaces was not dependent on the hydrophobicity of the materials. These studies revealed that bacterial adhesion is not always correlated with surface properties. It is also apparent that studies performed under different hydrodynamic conditions have led to different conclusions. Thus, the effects of surface properties on bacterial adhesion should be evaluated in different hydrodynamic conditions according to the intended use of that material.

In this study, the adhesion of *E. coli* to glass and PDMS under different flow rates was monitored in a PPFC in order to understand the combined effect of the hydrodynamic conditions and surface properties on initial bacterial adhesion. A better understanding of

the factors affecting the initial bacterial adhesion is important in the development of strategies to delay the onset of bacterial biofilms in biomedical devices.

Materials and methods

Numerical simulations

The PPFC used in the present work has a rectangular cross section of 0.8×1.6 cm and a length of 25.42 cm. The inlet and outlet tubes have a diameter (D_{in}) of 0.2 cm. The flow regime was defined using the Reynolds number calculated using the diameter and the velocity (V_{in}) of the inlet:

$$Re_{in} = \frac{\rho V_{in} D_{in}}{\mu}$$

Here ρ and μ are the density and viscosity of water, respectively.

A laminar regime in the inlet was considered for the flow rates of 1 and 2 ml.s^{-1} (Re_{in} < 2000), and a turbulent regime was assumed for the flow rates of 4, 6, 8 and 10 ml.s^{-1} (Re_{in} > 3500).

Numerical simulations were made in Ansys Fluent CFD package (version 14.5). A model of the PPFC was built in Design Modeller 14.5 and was discretized into a grid of 1,694,960 hexahedral cells by Meshing 14.5. The properties of water (density and viscosity) at 37 ºC were used for the fluid.

Results in the laminar regime were obtained by solving the Navier-Stokes equations. The velocity-pressure coupled equations were solved by the PISO algorithm [18], the QUICK scheme [19] was used for the discretization of the momentum equations and the PRESTO! scheme was chosen for pressure discretization. The no slip boundary condition was considered for all the walls. Results for the turbulent regime were obtained by solving the SST k-ω model [20] with low Reynolds corrections.

Simulations were made in transient mode, to assure convergence and to capture

transient flow structures. For each case, 2 s of physical time were simulated with a fixed time step of 10^{-4} s. Observation of the trajectories of tracer PVC particles circulating in the PPFC at different flow rates (as described in Teodósio, et al. [21]) confirmed the flow pathlines predicted by CFD (not shown). A mesh independence analysis was performed by using a mesh with 690,475 cells and a 4.9% variation was obtained in the wall shear stress. Despite the small variation, the more refined mesh was used in the simulations to increase numerical accuracy.

Bacteria and culture conditions

Escherichia coli JM109(DE3) was used since this strain had already demonstrated a good biofilm formation capacity [22]. A starter culture was prepared as described by Teodósio, et al. [23] and incubated overnight. A volume of 60 mL from this culture was centrifuged (for 10 min at 3202 *g*) and the cells were washed twice with citrate buffer 0.05 M [24], pH 5.0. The pellet was then resuspended and diluted in the same buffer to obtain a cell concentration of 7.6×10^{7} cell.mL^{-1}.

Surface preparation and flow chamber experiments

The PPFC was coupled to a jacketed tank connected to a centrifugal pump by a tubing system. The PPFC contained a bottom and a top opening for the introduction of the test surfaces of glass and PDMS. Glass slides were firstly washed by immersion in a glass beaker containing 60 ml of a 0.5% solution of detergent (Sonasol Pril, Henkel Ibérica S A) for 30 min. After this, the slides were rinsed (with a squeezing bottle) with distilled water (10 ml) to remove the detergent and then they were immersed in other beaker containing sodium hypochlorite (60 ml at 3%) for an additional 30 min. After rinsing again with 10 ml of distilled water, half of the slides were coated with PDMS.

The PDMS (Sylgard 184 Part A, Dow Corning) was submitted to a 30 min ultrasound treatment in order to eliminate all the bubbles. The curing agent (Sylgard 184 Part B, Dow Corning) was added to the PDMS (at a 1:10 ratio). PDMS was deposited as a thin layer (with a uniform thickness of 10 µm) on top of the glass slides by spin coating (Spin150 PolosTM) at 2000 rpm for 60 seconds.

The PPFC was mounted in a microscope (Nikon Eclipse LV100, Japan) to monitor cell attachment. The cellular suspension was circulated through the PPFC at 1, 2, 4, 6, 8 or 10 $ml.s^{-1}$ for 30 min. Images were acquired every 60 s with a camera (Nikon DS-RI 1, Japan) connected to the microscope. Temperature was kept constant at 37 ºC using a recirculating water bath connected to the tank jacket. Three independent experiments were performed for each surface and flow rate.

Surface hydrophobicity and free energy of adhesion

Bacterial and surface hydrophobicity (ΔG) and the free energy of adhesion (ΔG^{Adh}) were determined as described in van Oss [25] . Contact angles were measured at 25 ± 2 ºC in a contact angle meter (Dataphysics OCA 15 Plus, Germany) using water, formamide and α-bromonaphtalene (Sigma) as reference liquids. One *E. coli* suspension was prepared as described for the adhesion assay and its physicochemical properties were also determined by contact angle measurement as described by Busscher, et al. [26].

The Lifshitz-van der Waals components (γ^{LW}) and Lewis acid-base components (γ^{AB}) which comprises the electron acceptor γ^{+} and electron donor γ^{-} parameters were determined as described in van Oss [25] enabling the determination of ΔG and ΔG^{Adh}, using the equations:

$$\Delta G = -2\left(\sqrt{\gamma_s^{LW}} - \sqrt{\gamma_w^{LW}}\right)^2 + 4\left(\sqrt{\gamma_s^+\gamma_w^-} + \sqrt{\gamma_s^-\gamma_w^+} - \sqrt{\gamma_s^+\gamma_s^-} - \sqrt{\gamma_w^+\gamma_w^-}\right); \quad (1)$$

$$\Delta G^{Adh} = \gamma_{sb}^{LW} - \gamma_{sw}^{LW} - \gamma_{bw}^{LW} + 2\left[\sqrt{\gamma_w^+}\left(\sqrt{\gamma_s^-} + \sqrt{\gamma_b^-} - \sqrt{\gamma_w^-}\right) + \sqrt{\gamma_w^-}\left(\sqrt{\gamma_s^+} + \sqrt{\gamma_b^+} - \sqrt{\gamma_w^+}\right) - \sqrt{\gamma_s^+\gamma_b^-} - \sqrt{\gamma_s^-\gamma_b^+}\right] \quad (2)$$

If $\Delta G < 0$ mJ.m^{-2}, the material is considered hydrophobic, if $\Delta G > 0$ mJ.m^{-2}, the material is hydrophilic. If $\Delta G^{Adh} < 0$ mJ.m^{-2} adhesion is favoured, while adhesion is not expected to occur if $\Delta G^{Adh} > 0$ mJ.m^{-2}.

Data analysis

Microscopy images acquired in real time during the adhesion assays were analyzed with an image analysis software (ImageJ 1.46r) in order to obtain the number of adhered cells over time (30 min assay). The number of bacterial cells was then divided by the surface area of the field of view to obtain the number of cells per square centimeter. The ratio between the number of adhered cells on PDMS and glass was calculated for each time point and average values for the whole assay were determined for each flow rate.

The theoretical mass transport in a given flow displacement system can be calculated by solving the von Smoluchowski-Levich (SL) equation (approximate solution) which assumes that all microorganisms sufficiently close to the surface will adhere irreversibly [27]. Accordingly, a theoretical bacterial deposition rate (cells.m^{-2}.min^{-1}) can be calculated for the PPFC under the experimental conditions by:

$$SL = 0.538 \frac{D_\infty C_b}{R_b} \left(\frac{Pe\, h_0}{x}\right)^{1/3} \quad (3)$$

where D_∞ is the diffusion coefficient (approximately 4 x 10^{-13} m^2.s^{-1} for microorganisms), C_b is the bacterial concentration (cell.m^{-3}), R_b is the microbial radius

(m), h_0 is the height of the rectangular channel (m) and x is the distance for which an average velocity variation below 15 % was determined (m).

The equation includes the Péclet number (*Pe*) which represents the ratio between convective and diffusional mass transport, given for the parallel plate configuration as:

$$Pe = \frac{3v_{av}\ {R_b}^3}{2(h_0/2)^2 D_\infty} \quad (4)$$

where v_{av} is the average flow velocity (m.s^{-1}). Eq. 3 predicts the cell adhesion rates per surface area for a certain flow rate. From this value it is possible to calculate the number of adhered cells for each flow rate, multiplying the rate by the correspondent time point.

Statistical analysis

Paired *t*-test analyses were performed to evaluate if statistically significant differences were obtained with the two materials. Three independent experiments were performed for each surface and flow rate. Each time point was evaluated individually using the three independent results obtained with glass at one flow rate and the three individual results obtained with PDMS at the same flow rate. Results were considered statistically different for a confidence level greater than 95% ($P < 0.05$) and these time points were marked with an asterisk (*). Standard deviation between the 3 values obtained from the independent experiments was also calculated and average deviations below 17% and 21% were obtained for glass and PDMS respectively.

Results

Numerical simulation of the flow

Figure 1 shows the axial velocity (*x* component) in the midplane of the cell. For the laminar regimes, a laminar jet extends to a distance of about three quarters of the cell length (x = 0.19 m). The flow is transient, a result consistent with experimental

observations [28]. Transient vortices are formed along the cell between the jet and the wall. The jet may sometimes break into temporary vortices and recover its length again. However, the flow stabilizes as it approaches the viewing point where the conditions are of steady flow. Results for the turbulent regimes show a much shorter jet that slowly increases with increasing flow rate. The flow conditions in the viewing point are also stable. The highest flow velocity values are found in the inlet zone which is also the zone where highest flow velocity variations occur.

Figure 2 represents the distribution of wall shear stress along the cell. For the laminar cases, wall shear stress peaks are obtained where the jet breaks, due to the formation of vortices. For the turbulent cases, since the jets break at a shorter distance, the wall shear stress is higher for $x < 0.05$ m. In all cases (laminar or turbulent), the wall shear stress at the viewing point is stable. Wall shear stresses between 0.005 and 0.07 Pa (corresponding to shear strain rates between 7 and 100 s^{-1}, respectively) are obtained in the visualization zone in this PPFC for the flow rates studied.

Bacterial adhesion

A PPFC containing a glass or a PDMS surface was operated at six different flow rates in order to study the effect of the hydrodynamic conditions and surface properties on *E. coli* adhesion. The results in Table 1 show that glass and *E. coli* are both hydrophilic ($\Delta G > 0$ mJ.m^{-2}) and that PDMS is hydrophobic ($\Delta G < 0$ mJ.m^{-2}). Additionally, it is possible to observe that glass has the highest γ^{LW} value and PDMS the lowest. Regarding γ^{-} and γ^{+}, results showed that PDMS and *E. coli* are monopolar surfaces, being electron donors and glass is a polar surface, being an electron donor and acceptor. From a thermodynamic point of view, *E. coli* adhesion to PDMS and glass is not expected to occur ($\Delta G^{Adh} > 0$ mJ.m^{-2}). Additionally, *E. coli* adhesion to glass is less

favourable than to PDMS (ΔG^{Adh} glass > ΔG^{Adh} PDMS).

Figure 3 depicts the adhesion curves obtained for PDMS and glass for each flow rate. The number of adhered cells increased with time in all cases. Adhesion on PDMS (Figure 3a) was higher than on glass for 72% of the points ($P < 0.05$). Values were on average 2.4 fold higher than predicted by the SL solution. Regarding adhesion on glass, values obtained were on average 1.4 fold higher than predicted. For the flow rates of 2 and 4 $ml.s^{-1}$ (Figures 3b and 3c), the number of adhered cells on PDMS and glass was similar during the experimental time ($P > 0.05$) and the results agree with those predicted by the SL solution. In Figure 3d it is possible to observe that for a flow rate of 6 $ml.s^{-1}$, adhesion on PDMS was higher than on glass. Experimental results obtained for PDMS were on average 1.5 fold higher than predicted. Adhesion on glass was on average 1.4 fold higher than predicted for the first 17 min. However, after 17 min, the theoretical values were, on average, 1.2 fold higher than the experimental. With flow rates of 8 and 10 $ml.s^{-1}$ (Figures 3e and 3f) the number of adhered cells on PDMS was higher than on glass, in the first case for 55% of the time points and in the second for 93% of the points ($P < 0.05$). For both flow rates, during the first 13 min, the number of adhered cells on both surfaces was successfully predicted. From 13 min onwards, the number of adhered cells on PDMS was on average 1.4 fold lower than predicted. Regarding the glass surface, the SL solution predicted twice the amount of adhered cells than what was experimentally observed.

Figure 4 shows the average wall shear stress and the ratio between the number of adhered cells on PDMS and glass for each flow rate. For the lower flow rate (corresponding to a shear stress of 0.005 Pa), adhesion on PDMS was on average 1.7 fold higher than on glass ($P < 0.05$). Regarding the intermediate flow rates, 2 and 4 $ml.s^{-1}$, similar adhesion values were obtained for both surfaces ($P > 0.05$). For the

higher flow rates (6, 8 and 10 $ml.s^{-1}$) a higher number of adhered cells was observed on PDMS than on glass (although with no statistical significant difference for 6 $ml.s^{-1}$). It was observed that for shear stresses higher than 0.03 Pa, until a maximum of 0.07 Pa (between 4 and 10 $ml.s^{-1}$), an increase in shear stress amplified the difference between the two surfaces.

Discussion

A PPFC was used to assess the combined influence of six hydrodynamic conditions (flow rates between 1 and 10 $ml.s^{-1}$) and two surfaces, one hydrophilic (glass) and another hydrophobic (PDMS), on the initial adhesion of *E. coli*. Numerical simulations showed that under these flow rates, shear stresses between 0.005 and 0.07 Pa can be attained in the PPFC. Since wall shear stresses lower than 0.1 Pa can be found in the urinary system (eg bladder and urethra) [29], circulatory system (eg veins) [30] and reproductive system (eg uterus) [31], this platform can be used to simulate the hydrodynamic conditions found in different locations of the human body.

The process of bacterial adhesion can be affected by the hydrodynamic conditions but also by cell and surface properties [32]. It was observed that, in general, *E. coli* adhesion was higher on PDMS than on glass and this is in agreement with the thermodynamic theory since adhesion on hydrophilic (glass) surfaces is less favorable. Fletcher and Loeb [33] observed that the number of bacteria adhered on a surface is related to the surface charge and degree of hydrophobicity of the substratum. They verified that a higher number of marine *Pseudomonas sp.* cells adhered on hydrophobic surfaces than in hydrophilic materials. Cerca, et al. [34] studied the physicochemical interactions involved on the adhesion of 9 clinical isolates of *S. epidermidis* to different surfaces. They observed that adhesion to hydrophobic surfaces was favored for all strains when compared to hydrophilic surfaces.

With a flow rate of 1 $ml.s^{-1}$, the number of adhered cells on PDMS was higher than on glass, and for both surfaces this number was higher than predicted by the SL solution. In the SL approximation, bacterial mass transport is governed by diffusion and convection in the absence of gravitational, colloidal and hydrodynamic interactions [35, 36]. Experimental adhesion rates higher than those predicted by this model have been observed [37, 38]. These have been attributed to the contribution of sedimentation phenomena at lower flow rates [35] and to presence of surface appendages, e.g. flagellum, which may have a positive effect on adhesion, a feature that is also not considered in this model [39]. Li, et al. [35] have studied the contribution of sedimentation to mass transport in a PPFC using *S. aureus* and a glass surface. Having tested stagnant conditions and flow rates up to 0.33 $ml.s^{-1}$, these authors have shown that when accounting for sedimentation in calculating deposition efficiencies, these decrease with increasing flow rates. Although the flow rates used in this work are three to thirty fold higher than the highest flow rate used on that study it is possible that mass transport by sedimentation may have some importance particularly at the lowest flow rate tested. Bacterial appendages will allow bacteria to swim thus enhancing the rate of arrival to the surface [40]. When cells are sufficiently close to the surface, the interacting forces between them and the surface may govern the adhesion since differences in the number of adhered cells between PDMS and glass were observed. Wang, et al. [38] observed that after cells are transported to the substrate surface, the initiation of adhesion was dependent on the interaction energy between the cells and that surface. Bayoudh, et al. [41] compared the adhesion of *Pseudomonas stutzeri* and *S. epidermis* on two different surfaces. They observed that *P. stutzeri* used its surface structures to adhere more strongly and irreversibly on both surfaces, while *S. epidermis* adhered reversibly and this was dependent on the surface energy barrier. However, both

bacterial strains adhered in higher numbers to hydrophobic surfaces when compared to hydrophilic materials.

With flow rates of 2 and 4 $ml.s^{-1}$, the number of adhered cells was similar for both surfaces and the values were successfully predicted by the SL solution. This theory considers that bacterial adhesion will increase with increasing flow velocities, due to the increased cell transport to the surface. However, the model does not account for the fact that a higher flow rate promotes higher shear stresses that may prevent cellular attachment [42]. This hindrance may be overcome by the bacterial appendages used in adhesion [43]. Moreover, since these structures have a small size, they can help to overcome the energy barrier between the bacteria and the surface and facilitate adhesion [44]. Thus, with a stronger shear stress, the first interaction between cells and surface may be mediated directly by the cellular appendages [29, 38]. Therefore, a balance between the negative effect of the shear forces and the positive effect of the cellular appendages may be achieved. Although none of these factors is accounted for in the SL solution, they can cancel one another and therefore bacterial adhesion was successfully predicted by the model under these conditions.

Regarding the results obtained for a flow rate of 6 $ml.s^{-1}$, it was possible to observe that a higher number of cells adhered on PDMS than on glass. The number of adhered cells on PDMS was slightly higher than predicted and the same was observed for glass for the first 17 min of the assay. However, after this initial period, the number of adhered cells on glass was lower than predicted by the SL solution indicating that some type of blocking may have occurred. Under a higher flow velocity, the number of cells arriving to the surface is higher and cellular appendages may contribute to a higher productivity in adhesion [42, 44]. However, since a stronger shear stress is promoted under this hydrodynamic condition and a lower contact time between the cells and the surface is expected, the gliding motion along the surface, which can happen during reversible

adhesion, may be hampered [42, 45]. Thus, the adhesion step must be quicker in order to overcome this effect. In the first minutes, cells have all the surface free to adhere. However, after some minutes some areas become occupied by adhered cells thus reducing the free area available for attachment [37]. For a flow rate of 6 $ml.s^{-1}$, it seems that this blocking effect starts at 17 min only for the glass surface. This effect was not observed for the PDMS surface, indicating that surface properties also have an important role in bacterial adhesion in this condition. Knowing that adhesion on glass is less favorable according to the thermodynamic theory it is possible that both factors (thermodynamic and the blocking effect) may inhibit adhesion to this surface.

At higher flow rates (8 and 10 $ml.s^{-1}$), although a higher adhesion was predicted by the model, a lower number of adhered cells was observed for both surfaces. This may be due to the increased shear stress, the decreased contact time with the surface, the blocking effect, or even desorption promoted by bacterial collisions [46, 47]. Lecuyer, et al. [48] investigated the influence of the wall shear stress in the adhesion of *P. aeruginosa*. They verified that the number of binding events decreased as the shear stress increased in a range of wall shear stresses between 0.05 and 10 Pa. Shive, et al. [49] studied the effect of shear stresses between 0 and 1.75 Pa in the adhesion of *S. epidermidis* and leukocytes to polyetherurethane. They observed that adhesion decreased with increasing shear stress. In this work, with the two higher flow rates tested, it was also observed that bacterial adhesion was different between the two surfaces indicating that surface properties affected adhesion. A lower number of adhered cells was observed on glass than on PDMS and these values were lower than theoretically predicted. It seems that with these flow rates the stronger shear stresses had a higher inhibitory effect on cellular adhesion on glass, which is the surface that is theoretically less favorable for adhesion. Regarding the PDMS surface, it was observed that until 13 min, the SL solution was able to predict the number of adhered cells. After

13 min, the number of adhered cells on PDMS was lower than the values predicted by the SL solution indicating that a blocking effect may be occurring. The surface coverage for this condition was estimated as described by Adamczyk, et al. [50] to be approximately 3%. Li, et al. [51] have studied *S. aureus* adhesion to glass at a comparable shear rate (84 s^{-1}) and did not find any significant blocking effects at a surface coverage of approximately 10%. It is however plausible that this effect is dependent on the bacteria and surface that is used for the assays. When PDMS is used as substrate, since this surface is thermodynamically more favorable for adhesion, the inhibitory effect caused by the shear stress is only noticed after 13 min possibly due to the reduction of free area available for adhesion and the lower contact time between the cells and the surface, which may hamper the adhesion assistance effect provided by the cellular appendages [43].

The use of modified materials or polymeric coatings with enhanced surface properties is a promising strategy to inhibit bacterial colonization of surfaces in the biomedical sector [1, 52, 53]. Although some encouraging results have been obtained both *in vitro* and *in vivo* [54], one has to bear in mind that these modified materials with enhanced properties are often much more expensive than the original materials from which they are derived. The results presented in this study demonstrate that *E. coli* adhesion to both hydrophilic and hydrophobic surfaces is modulated by shear stress. Depending on the prevailing hydrodynamic conditions, the effect of surface properties on bacterial adhesion is either more noticeable or less important than the effect of the shear forces. This suggests that when materials are selected to produce biomedical devices or when coatings are developed for surface protection against biofilm formation, the knowledge of the shear stress field that will exist during the *in vivo* use of these devices may be very important. Thus, depending on the hydrodynamic regime that is found in each particular application, the use of more expensive materials or polymeric coatings may

be justified or not.

Acknowledgments

The authors acknowledge the financial support provided by COMPETE, FEDER and by FCT through Projects PTDC/EBB-BIO/104940/2008 and PTDC/EQU-FTT/105535/2008.

References

[1] P. Kaali, E. Strömberg and S. Karlsson, in A.N. Laskovski (Eds.), Prevention of biofilm associated infections and degradation of polymeric materials used in biomedical applications, InTech, 2011, 22.

[2] Y.L. Ong, A. Razatos, G. Georgiou and M.M. Sharma, Langmuir, 15 (1999) 2719-2725.

[3] T. Shunmugaperumal (Eds.), Biofilm eradication and prevention: a pharmaceutical approach to medical device infections, Wiley, New Jersey, 2010.

[4] D. Aubert, Prog Urol, 20 (2010) 251-259.

[5] M.H. Castonguay, S. van der Schaaf, W. Koester, J. Krooneman, W. van der Meer, H. Harmsen and P. Landini, Res Microbiol, 157 (2006) 471-478.

[6] B.W. Trautner, A.I. Lopez, A. Kumar, D.M. Siddiq, K.S. Liao, Y. Li, D.J. Tweardy and C. Cai, Nanomed Nanotechnol, 8 (2012) 261-270.

[7] H. Koseoglu, G. Aslan, N. Esen, B.H. Sen and H. Coban, Urology, 68 (2006) 942-946.

[8] M. Wood, Community Eye Health, 12 (1999) 19-20.

[9] J.L. Pace, M.E. Rupp and R.G. Finch (Eds.), Biofilms, Infection and Antimicrobial Therapy, CRC pres Taylor and Francis group, Boca Raton, 2006.

[10] J.D. Bryers, Biotechnol Bioeng, 100 (2008) 1-18.

[11] H.J. Busscher, H.C. van der Mei, G. Subbiahdoss, P.C. Jutte, J.J.A.M. van den Dungen, S.A.J. Zaat, M.J. Schultz and D.W. Grainger, Sci Transl Med, 4 (2012) 153rv110.

[12] Y. Nikolaev and V. Plakunov, Microbiology, 76 (2007) 125-138.

[13] J.S. Teodósio, M. Simões, L. Melo and F.J. Mergulhão, in M. Simões, F.J. Mergulhão (Eds.), Platforms for in vitro biofilm studies, Nova science publishers 2013, 3.

[14] A.J. Barton, R.D. Sagers and W.G. Pitt, J Biomed Mater Res, 30 (1996) 403-410.

[15] I.H. Pratt-Terpstra, A.H. Weerkamp and H.J. Busscher, Journal of General Microbiology, 133 (1987) 3199-3206.

[16] G.M. Bruinsma, H.C. van der Mei and H.J. Busscher, Biomaterials, 22 (2001) 3217-3224.

[17] K.W. Millsap, G. Reid, H.C. van der Mei and H.J. Busscher, Biomaterials, 18 (1997) 87-91.

[18] R.I. Issa, J Comput Phys, 62 (1986) 40-65.

[19] B.P. Leonard, Comput Meth Appl Mech Eng, 19 (1979) 59-98.

[20] F.R. Menter, AIAA J, 32 (1994) 1598-1605.

[21] J.S. Teodósio, M. Simões, M.A. Alves, L. Melo and F. Mergulhão, The Scientific World Journal ID 361496 (2012).

[22] J.S. Teodósio, M. Simões and F.J. Mergulhão, J Appl Microbiol, 113 (2012) 373–382.

[23] J.S. Teodósio, M. Simões, L.F. Melo and F.J. Mergulhão, Biofouling, 27 (2011) 1-11.

[24] M. Simões, L.C. Simões, S. Cleto, M.O. Pereira and M.J. Vieira, Int J Food Microbiol, 121 (2008) 335-341.

[25] C. van Oss (Eds.), Interfacial Forces in Aqueous Media, Marcel Dekker Inc., New

York, USA., 1994.

[26] H. Busscher, A. Weerkamp, H.v.d. Mei, A. Pelt, H. Jong and J. Arends, Appl Environ Microbiol, 48 (1984) 980-983.

[27] M. Elimelech, Separations Technol, 4 (1994) 186-212.

[28] V. Todde, P. Spazzini and M. Sandberg, Exp Fluids, 47 (2009) 279-294.

[29] P. Aprikian, G. Interlandi, B.A. Kidd, I. Le Trong, V. Tchesnokova, O. Ykovenko, M.J. Whitfield, E. Bullitt, R.E. Stenkamp, W.E. Thomas and E. Sokurenko, PLoS Biol, 9 (2011).

[30] J.M. Ross, B.R. Alevriadou and L.V. McIntire, in Loscalzo J, A.I. Schafer (Eds.), Rheology, Williams & Wilkins, Baltimore, MD, 1998, 17.

[31] E.A. Nauman, C.M. Ott, E. Sander, D.L. Tucker, D. Pierson, J.W. Wilson and C.A. Nickerson, Appl Environ Microbiol, 73 (2007) 699-705.

[32] H. Wang, M. Sodagari, Y. Chen, X. He, B.-m.Z. Newby and L.-K. Ju, Colloids Surf B Biointerfaces, 87 (2011) 415-422.

[33] M. Fletcher and G.I. Loeb, Appl Environ Microbiol, 31 (1979) 67-72.

[34] N. Cerca, G.B. Pier, M. Vilanova, R. Oliveira and J. Azeredo, Res Microbiol, 156 (2005) 506-514.

[35] J. Li, H.J. Busscher, W. Norde and J. Sjollema, Colloids Surf B Biointerfaces, 84 (2011) 76-81.

[36] H.J. Busscher and H.C. van der Mei, Clin Microbiol Rev 19 (2006) 127-141.

[37] D.P. Bakker, H.J. Busscher and H.C. van der Mei, Microbiology, 148 (2002) 597-603.

[38] H. Wang, M. Sodagari, L.-K. Ju and B.-m. Zhang Newby, Colloids Surf B Biointerfaces, 109 (2013) 32-39.

[39] H. Morisaki, S. Nagai, H. Ohshima, E. Ikemoto and K. Kogure, Microbiology, 145 (1999) 2797-2802.

[40] V.B. Tran, S.M.J. Fleiszig, D.J. Evans and C.J. Radke, Appl Environ Microbiol, 77 (2011) 3644-3652.

[41] S. Bayoudh, A. Othmane, L. Mora and H. Ben Ouada, Colloids Surf B Biointerfaces, 73 (2009) 1-9.

[42] D.P. Bakker, A. van der Plaats, G.J. Verkerke, H.J. Busscher and H.C. van der Mei, Appl Environ Microbiol, 69 (2003) 6280-6287.

[43] J.W. McClaine and R.M. Ford, Biotechnol Bioeng, 78 (2002) 179-189.

[44] J. Sjollema, H.C. Van Der Mei, H.M.W. Uyen and H.J. Busscher, J Adhes Sci Technol, 4 (1990) 765-777.

[45] O.E. Petrova and K. Sauer, J Bacteriol, 194 (2012) 2413–2425.

[46] J.M. Meinders and H.J. Busscher, Langmuir, 11 (1995) 327-333.

[47] T. Dabros and T.G.M. van de Ven, Colloids Surf A Physicochemical and Engineering Aspects, 75 (1993) 95-104.

[48] S. Lecuyer, R. Rusconi, Y. Shen, A. Forsyth, H. Vlamakis, R. Kolter and H.A. Stone, Biophys J 100 (2011) 341-350.

[49] M.S. Shive, S.M. Hasan and J.M. Anderson, J Biomed Mater Res A 46 (1999) 511-519.

[50] Z. Adamczyk, B. Senger, J.-C. Voegel and P. Schaaf, J Chem Physics, 110 (1999) 3118-3128.

[51] J. Li, H.J. Busscher, H.C. van der Mei, W. Norde, B.P. Krom and J. Sjollema, Colloids Surf B Biointerfaces, 87 (2011) 427-432.

[52] J. Tsibouklis, M. Stone, A.A. Thorpe, P. Graham, V. Peters, R. Heerlien, J.R. Smith, K.L. Green and T.G. Nevell, Biomaterials, 20 (1999) 1229-1235.

[53] D. Campoccia, L. Montanaro and C.R. Arciola, Biomaterials, 34 (2013) 8533-8554.

[54] T. Coenye and H.J. Nelis, Journal of Microbiological Methods, 83 (2010) 89-105.

Table 1 Contact angle measurements (θ), the apolar (γ^{LW}) and polar (γ^{AB}) components, the surface tension parameters (γ^{+} and γ^{-}), the hydrophobicity (ΔG) of both surfaces and *E. coli* cells and the free energy of adhesion (ΔG^{Adh}) between *E. coli* and each surface

Surface	Contact angle / º			γ^{LW} / (mJ.m^{-2})	γ^{+} / (mJ.m^{-2})	γ^{-} / (mJ.m^{-2})	γ^{AB}/ (mJ.m^{-2})	ΔG / (mJ.m^{-2})	ΔG^{Adh}/ (mJ.m^{-2})
	θ_w	θf_{orm}	θ_{br}						
Glass	16.4 ±0.3	44.5 ±0.7	17.2 ±0.3	32.6	2.6	52.4	23.3	28.0	62.9
PDMS	113.6 ±0.6	87.6 ±1.8	111.2 ±0.6	12.0	0.0	4.5	0.0	-61.8	32.6
E. coli	19.1 ±0.9	58.5 ±2.0	73.3 ±0.7	25.7	0.0	123.2	0.0	121.9	-

Figure captions

Figure 1 Absolute velocity in the midplane of the cell.

Figure 2 Wall shear stress in the bottom wall of the cell.

Figure 3 Adhesion of *E. coli* on PDMS (open symbols), on glass surfaces (closed symbols) and the theoretical values predicted by the von Smoluchowski-Levich (SL) approximate solution (line), during 30 min for each flow rate: a) 1 $ml.s^{-1}$, b) 2 $ml.s^{-1}$, c) 4 $ml.s^{-1}$, d) 6 $ml.s^{-1}$, e) 8 $ml.s^{-1}$, f) 10 $ml.s^{-1}$. These results are an average of those obtained from three independent experiments for each condition. Statistical analysis corresponding to each time point is represented with an * for a confidence level greater than 95% ($P < 0.05$).

Figure 4 Ratio between *E. coli* adhesion on PDMS and glass surfaces (circles) for different flow rates and average wall shear stress for each flow rate determined by CFD (triangles). A solid line was drawn to highlight the points where *E. coli* adhesion results are similar on both surfaces. These results are an average of those obtained from three

independent experiments for each surface and flow rate.

Figure 1
Click here to download high resolution image

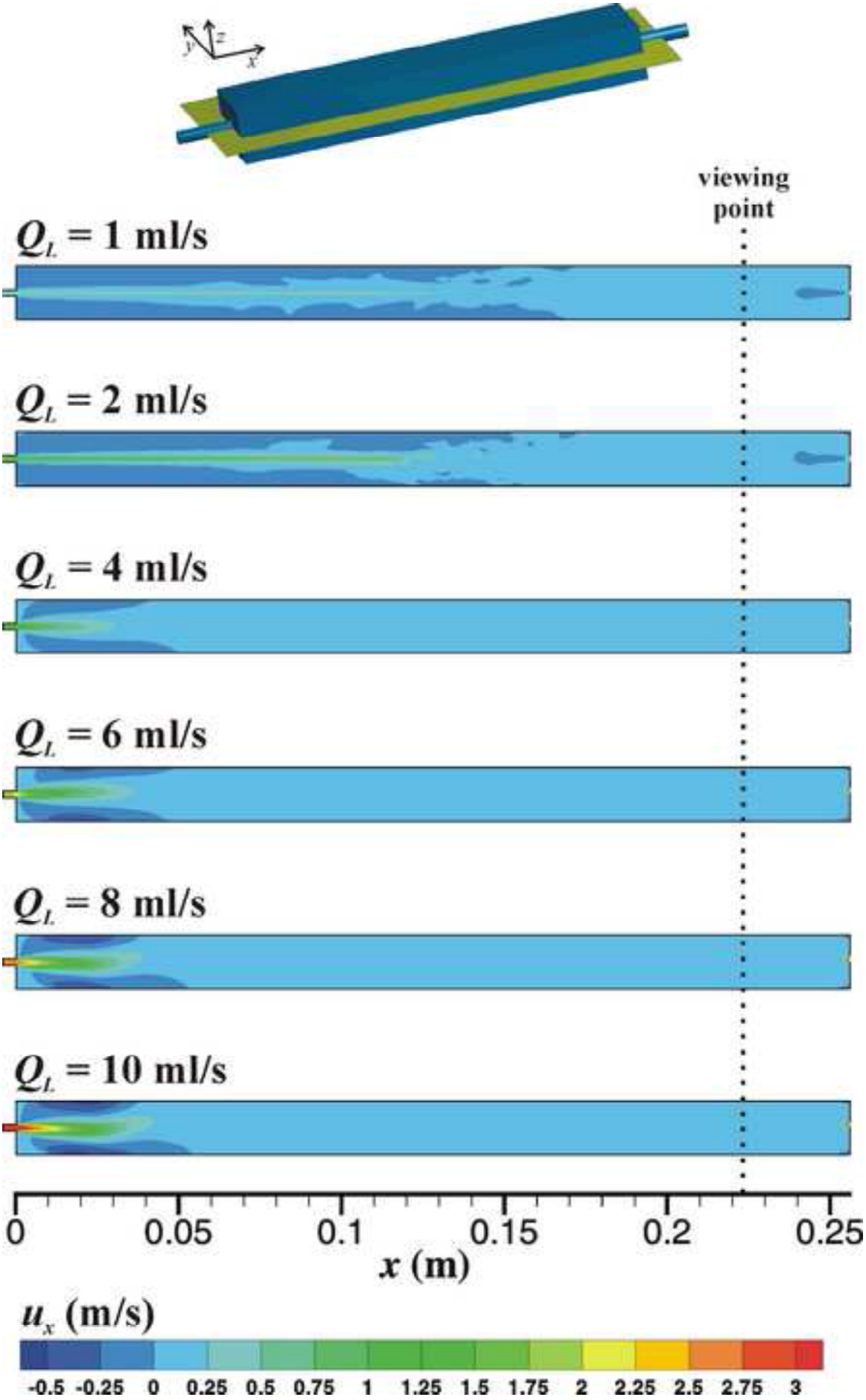

Figure 2
Click here to download high resolution image

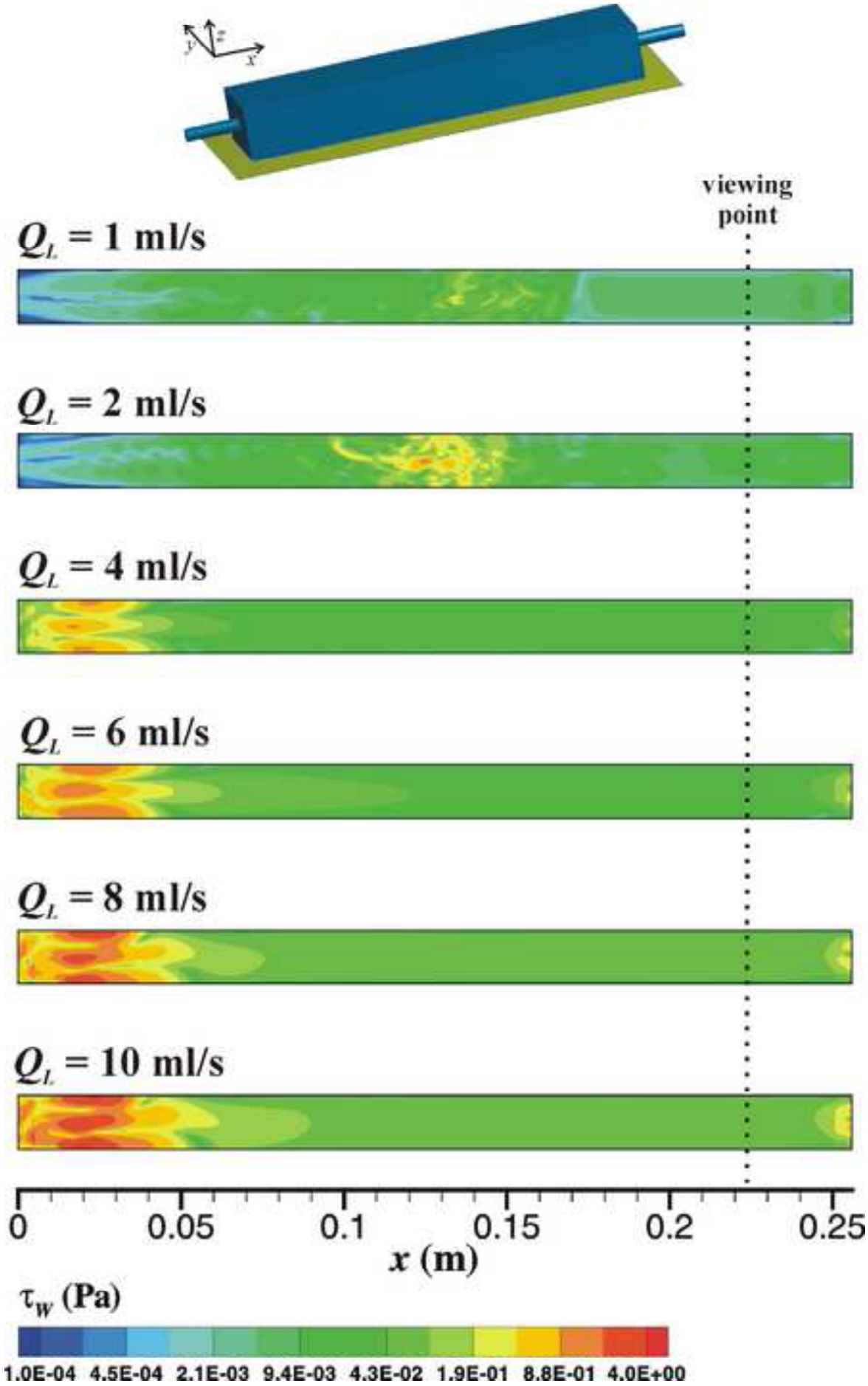

Figure 3
Click here to download high resolution image

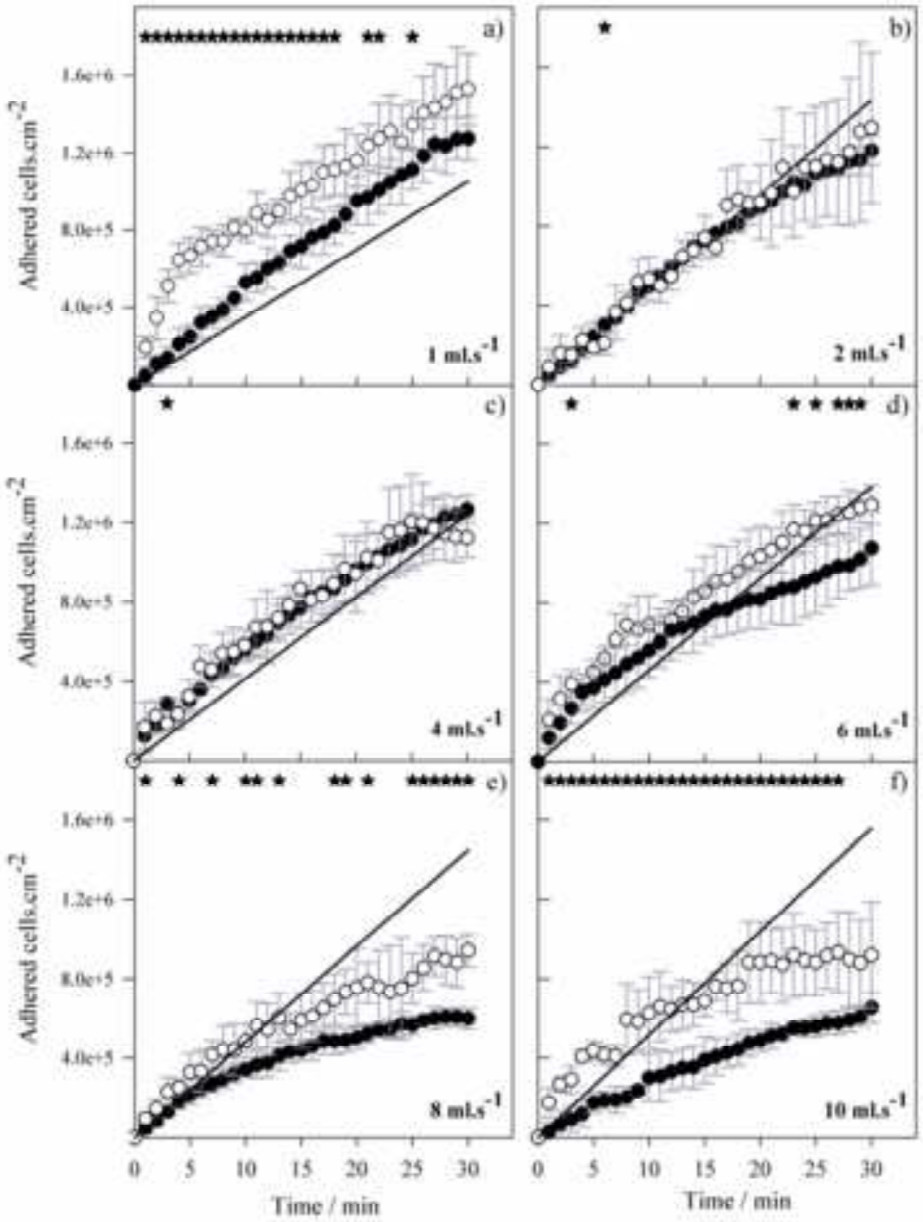

Figure 4
Click here to download high resolution image

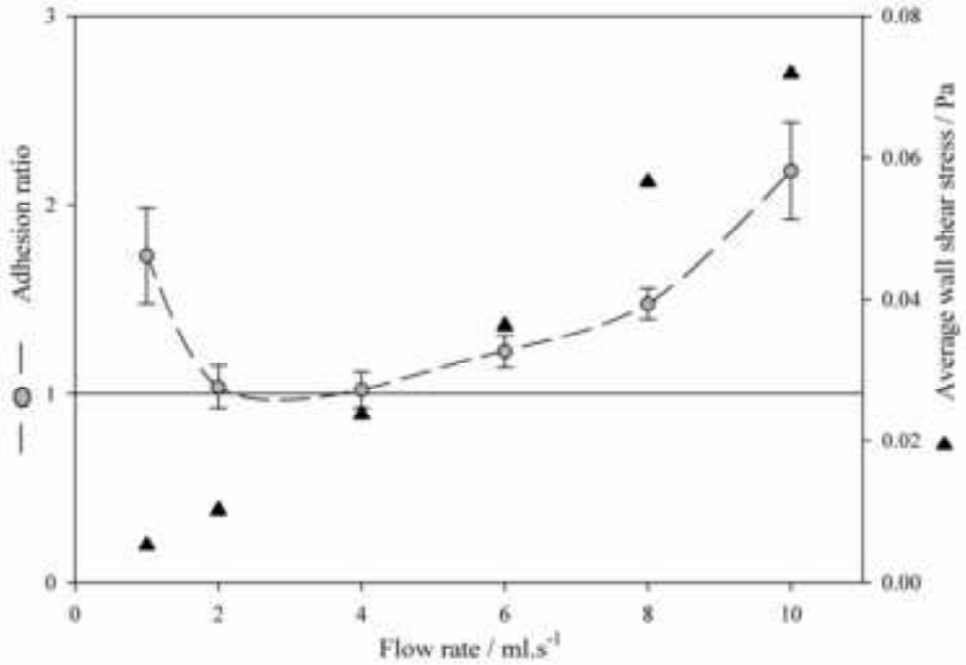

***Highlights (for review)**

Highlights

The combined effects of surface properties and hydrodynamic conditions on *Escherichia coli* adhesion were evaluated using a parallel plate flow chamber.
Surface properties only affected adhesion at the lowest and highest shear stresses tested and no effect was found at intermediate levels.
When expensive materials are selected to produce biomedical devices, the local hydrodynamic conditions should be taken into account.
Shear stress values obtained in this parallel plate flow chamber are similar to those found in circulatory, reproductive and urinary systems.

***Graphical Abstract (for review)**